Journal of Geodesy (2021) 95:57
https://doi.org/10.1007/s00190-021-01513-9

ORIGINAL ARTICLE

Quantification of corrections for the main lunisolar nutation components and analysis of the free core nutation from VLBI-observed nutation residuals

Ping Zhu[1] · Santiago Andrés Triana[1] · Jerémy Rekier[1] · Antony Trinh[2] · Véronique Dehant[1]

Received: 28 June 2020 / Accepted: 9 April 2021

Abstract
The attempt to quantify the corrections of lunisolar nutation components was made after analysis of six sets of Earth's orientation parameters (EOP). The deviations of the long-term nutation components about IAU2006/IAU2000A precession–nutation model are consistent with the uncertainties suggested by Mathews et al. (J Geophys Res Solid Earth, 2002. https://doi.org/10.1029/2001JB000390), but they exceed the errors determined in this work. The corrections are validated using the IERS 14C04 and IVS 19q4e combined solutions. After applying the corrections found in this work to the 14C04 nutation residuals, we analyzed the remaining signals, which contain the signature of the free core nutation (FCN). The eigenperiod of the FCN is fixed to the value derived from the resonance of the non-hydrostatic earth model in a priori. The amplitude of FCN is computed by fitting observations to the empirical model using a sliding window, the length of window is determined by taking into account the interference between those close nutation components and the FCN. In addition, we also fitted the nutation residuals by a viscous damping function; both methods produce the same results in the amplitudes of FCN. The magnitude of the free core nutation bears a "V-shape" distribution, and furthermore, the oscillation of the FCN shows a decay and a steady reinforcement before and after 1999. In order to examine the origin of the modulation in FCN's magnitude, we briefly analyzed the possible damping or beating mechanism behind it. We diagnosed the magnitude and running phase changes of FCN by comparing it with the occurrence of the transient geomagnetic jerks. The weighted root mean square errors of nutation residuals are minimally reduced about 36% when the corrections to the 21 nutation components and the FCN signature are considered together.

Keywords Nutation · Free core nutation · VLBI

1 Introduction

The torque induced by the Moon, the Sun, and the other planets are precisely known; the response of the rigid Earth to these external torques (Moon, Sun, and planets) deviates slightly from that of a pure solid body because of complicated geophysical processes involving the seasonal mass circulation of the atmosphere and ocean, the deformable mantle, the presence of a liquid outer core and solid inner core plus the coupling mechanisms at their interfaces. Very Long Baseline Interferometry (VLBI) technique is the most accurate way to measure the celestial pole offset (CPO), which are observed differences between the conventional model for the precession–nutation corrections of the CIP (Celestial Intermediate Pole) and the direction of the celestial pole observed using VLBI.

In practice, the conventional initial precession and nutation model is constructed based on a simplified solid Earth model (Kinoshita 1977). The IAU1980 nutation series (Seidelmann 1982) are developed from an elastic rotational oceanless Earth model (Wahr 1981). In those products, the contribution from planetary gravitational attraction is neglected, but it has been introduced after nearly at the same time by other efforts (Roosbeek and Dehant 1998; Bretagnon et al. 1998; Hartmann et al. 1999); the precision of all those series is truncated at the level of a tenth of a μas. With the accumulated VLBI observations, the discrepancy

✉ Ping Zhu
ping.zhu@observatoire.be

[1] Royal Observatory of Belgium, Av. Circulaire 3, 1180 Brussels, Belgium

[2] Lunar and Planetary Laboratory, University of Arizona, Tucson, AZ, USA

Published online: 23 April 2021

between the observations and the nutation series IAU1980 was significant. The deviation with respect to the IAU1980 nutation series has been investigated by several authors with the VLBI measured Earth's nutation (Herring et al. 1991). Zhu et al. (1990) apply the covariance analysis method, in which 106 nutation terms were fitted to find the corrections to the IAU1980 series (Zhu et al. 1990). The root mean square errors between this series and the IAU1980 are around 51 mas and 31 mas, corresponding to the changes in longitude and obliquity, respectively.

Herring et al. (2002) estimated the corrections for 21 major nutation terms w.r.t. the IAU1980 nutation model and the secular trends in longitude and obliquity w.r.t. the IAU1977 precession rate from a combined series by GSF and USNO, which cover the observation period from 1980 to 2000. They found the standard deviation (SD) of the nutation amplitudes with a period shorter than 400 days is 5 μas, and a value of 38 μas for the period longer than 400 days when numerical results were compared with the MHB2000 nutation series inferred from a set of basic Earth parameters (BEP) (Mathews et al. 2002; Herring et al. 2002). The amplitudes of the MHB2000 nutation components are obtained by convolving a designed transfer function with the rigid Earth model REN2000 (Souchay et al. 1999). The MHB2000 uses the VLBI observation fitted series (Herring et al. 2002) as input to systematically estimate the various effects such as the indirect loading and the core mantle couplings. This series was adopted by IAU as the IAU2000 nutation model (Soffel et al. 2003). The correction to the precession rate is discussed w.r.t. IAU2000 values by Capitaine et al. (2003), and it has been updated as the IAU2006 precession model, which has improved polynomial expressions for the precession of the ecliptic and the equator. These initiatives have led to a new adopted model the IAU2006/2000A based on the precession determined by Capitaine et al. (2003) and on nutation model or a non-rigid Earth as determined by Mathews et al. (2002). The IAU2006/IAU2000A precession–nutation model is composed of 678 lunisolar and 687 planetary terms induced by the gravitational attraction from the Moon, the Sun, and the other planets. The Basic Earth Parameters mainly includes the dynamic flattening of the core, the coupling constants at the core mantle boundary and several compliances (Mathews et al. 2002; Herring et al. 2002). The BEPs were estimated again from a longer series by Bayesian inversion (Koot et al. 2008). A comparison using the both methods has been provided recently (Zhu et al. 2017), re-estimating the parameters.

In this work, instead of estimating a new transfer function, corrections of two times 21 lunisolar nutation component are determined from the latest EOP provided by various independent analysis centers; totally it accounts for 42 terms in the nutation series. We start with eleven EOP solutions, removing five sets of data due to the large gap in the time series or due to higher noise level than the rest of data. The full name and location of the all eleven data analysis centers are given at Table 2. By analyzing jointly the six remaining EOP series, we determine the corrections for the 21 major nutation residuals components. The amplitudes associated with the correction of each term are determined from all the six EOP solutions. After recombining those values with the other nutation components from the IAU mode, these two times 21 new nutation amplitudes can be used to compute a new nutation series in longitude and obliquity or as celestial pole offsets that we call Fits20 and that is available on an internet repository under the name of Earth's NuTAtion (ENTA) (Zhu et al. 2020). We can then compare them with the IAU2006/2000A nutation series by using the IERS and IVS combined solutions.

After correcting those components from the IERS 14C04 nutation residuals dX and dY, we analyze the signature of the free core nutation (FCN). The eigenperiod of the FCN is fixed to the −430 solar days from the previous determination based on the analysis of the resonance effect in the transfer function made by Dehant et al. (2003), Koot et al. (2008) and Zhu et al. (2017). We then determine the amplitudes of the FCN mode on dX and on dY components, which correspond to the coefficients of real and imaginary part of the FCN mode, using sliding windows as it was done previously (Herring et al. 2002; Lambert 2006); meanwhile, we fitted the amplitude of the FCN by involving excitation and a viscous damping function after. The perturbation in the angular velocity, the decaying rate and the magnitude of the FCN are discussed by comparing it with a simplified viscous damping mechanism, with the possible beat between two modes and with the occurrence of the geomagnetic jerks in the end. In general, the weighted root mean square errors (wrms) are computed about IAU2006/2000A and Fits20 and FCN removed residuals (Table 1). The method to find the corrections to the 21 nutation component listed in the IAU2006/2000A is explained in Sects. 2 and 3. The way to fit the FCN is discussed separately in Sect. 4.

2 VLBI-determined global Earth Orientation Parameters

The data used in this work came from the following two sources: the international Earth Rotation Systems Service (IERS) and the Crustal Dynamics Data Information System (CDDIS), National Aeronautics and Space Administration (NASA). The EOP 14C04 are obtained through the IERS (www.iers.org). The 14C04 is aligned to the ITRF 2014 (Altamimi et al. 2016) and the ICRF2 the most recent versions of the conventional reference frames (Bizouard et al. 2018); a recent update on the reference frame has been introduced by Charlot et al. (2020). The IVS 19q4e is provided by

Table 1 The wrms is computed with the IERS (♭:14eopc04) and IVS (♮:ivs19q4e) combined solution, the unit of wrms is μas

Period	IAU	Fits20	FCN	IAU	Fits20	FCN	Size
1984–2020♭	171.7	161.0	108.8	175.1	163.5	106.1	13,465
1984–1999♭	177.2	173.7	148.8	170.6	162.5	132.2	5820
2000–2020♭	170.1	156.3	91.5	176.6	163.7	95.6	7645
1984–2020♮	173.2	154.1	68.9	173.9	160.7	71.0	4216
1984–1999♮	112.9	125.3	96.6	150.9	137.6	107.7	1501
2000–2020♮	175.0	155.7	66.8	175.0	161.9	68.1	2715

The wrms is repeatedly computed with the IAU2006/2000A model, with the Fits20 series, and after applying the corrections found in Fits20 plus the FCN signature determined from the empirical model using the 8-year sliding windows

Table 2 The name of the each VLBI center and their locations is listed

ASI	Space Geodesy Center Matera, Italy
BKG	Federal Agency for Cartography and Geodesy (BKG Leipzig) and Institute of Geodesy and Geoinformation of the University of Bonn (IGGB), Germany
CGS	Space Geodesy Center, Matera, Italy
GSF	NASA Goddard Space Flight Center, USA
OPA	Observatoire de Paris, France
SHA	Shanghai Observatory, China
USN	United States Naval Observatory, USA
AUS	GEOSCIENCE AUSTRALIA (AUS), Australia
IAA	Institute of Applied Astronomy, OCCAM/GROSS, Russia
SPU	Saint-Petersburg University, Russia
MAO	Main Astronomical Observatory, National Academy of Sci. of Ukraine (MAO NASU), Ukraine
IVS	International VLBI Service
IERS	International Earth Rotation and Reference Systems Service

the International VLBI Service for Geodesy and Astrometry solutions (IVS). Both IVS and IERS provide combined EOP solutions. The rest of global EOP solutions are from online archives of the Crustal Dynamics Data Information System CDDIS. All the data sets can be found online at the IERS or the CDDIS website (www.iers.org and ftp://cddis.gsfc.nasa.gov/vlbi). The full name and location of the all eleven data center are given in Table 2. More detailed information about each analysis center that provided a global EOP solution is listed in Table 3.

Importantly, differences exist in the ways each analysis center selects VLBI observation sessions, in the software used, and in the techniques applied to correct the local environmental effects that are also not exactly the same. However, concerning the nutation model, all the analysis centers employ the IAU2006/IAU2000A precession–nutation model as a priory. This suggests that the discrepancies in the amplitude of each nutation term, which has been derived from different centers, could originate from the following two sources: inconsistencies in the data used and differences in the data processing.

The nutation residuals are built from the IAU2006/2000A precession nutation model and from the global deployed VLBI stations, which are continuously monitoring radio waves emitted from the quasars. In the processing, the motions of the VLBI stations, such as the non-rigid Earth tides, have been corrected for. Additionally, the other effects such as deformation induced by atmosphere, ocean, and seismic activities have been taken into account by each center. These procedures are summarized in Table 3. After the processing of the VLBI data, final series of Earth Orientation Parameters (EOP) are obtained, which can be used as such or be combined in a next step to produce new series available at the international reference center such as IERS and IVS. The nutation residuals can bring valuable information to study the stability of the quasars and evaluate the international celestial reference frame, and probe the interior of the Earth (Dehant and Mathews 2015). The nutation residuals from IERS 14C04 and IVS 19q4e are plotted in Fig. 1. The IERS 14C04 data set is covering a period from January 1984 to December 2020 with 13,465 samples and the IVS solution is from November 1984 until October 2020 with 4216 solutions, respectively.

The corrections to the nutation component are reported by the study of Gattano et al. (2017) and Belda et al. (2017). The root-mean-square (RMS) error after correcting the nutation

Table 3 To retrieve the global EOP from VLBI measured time delay, a various of local environmental effects need to be corrected

Antenna thermal deformation:	Model Nothnagel 2008
Tropospheric delay:	VMF1, NMF dry mapping function Saastamoinen
Zenith delay:	Calculated using logged pressure, temperature; a priori mean gradients from DAO weather model
Tides:	Solid earth tides, pole tides, IERS conversion 1996/2000/2003/2006
Atmosphere loading:	Atmospheric pressure loading time series provided by the Goddard VLBI group NCEP Reanalysis model
Ocean loading:	FES2004 Hardisp model based on TPXO7.2 model GOT00.2 Ocean tide model
Post-seismic deformation correction:	exponential transient functions of the form $A(1-\exp((t-t_0)/\tau)$ a logarithmic functions of the form $A\log(1+(t-t_0)/\tau))$
Others:	The observation durations shorter than 18 h were not used. The data of sources which have two gravitational lenses and less than 4 good observations in all sessions were excluded
Software:	Calc/Solve. Version 9, 10 or 11 (ASI, BKG , CGS, GSF, OPA, SHA, USN) Occam 3.5, 6.2, GROSS (AUS, IAA, SPU); SteelBreeze-2.0.2 (MAO)

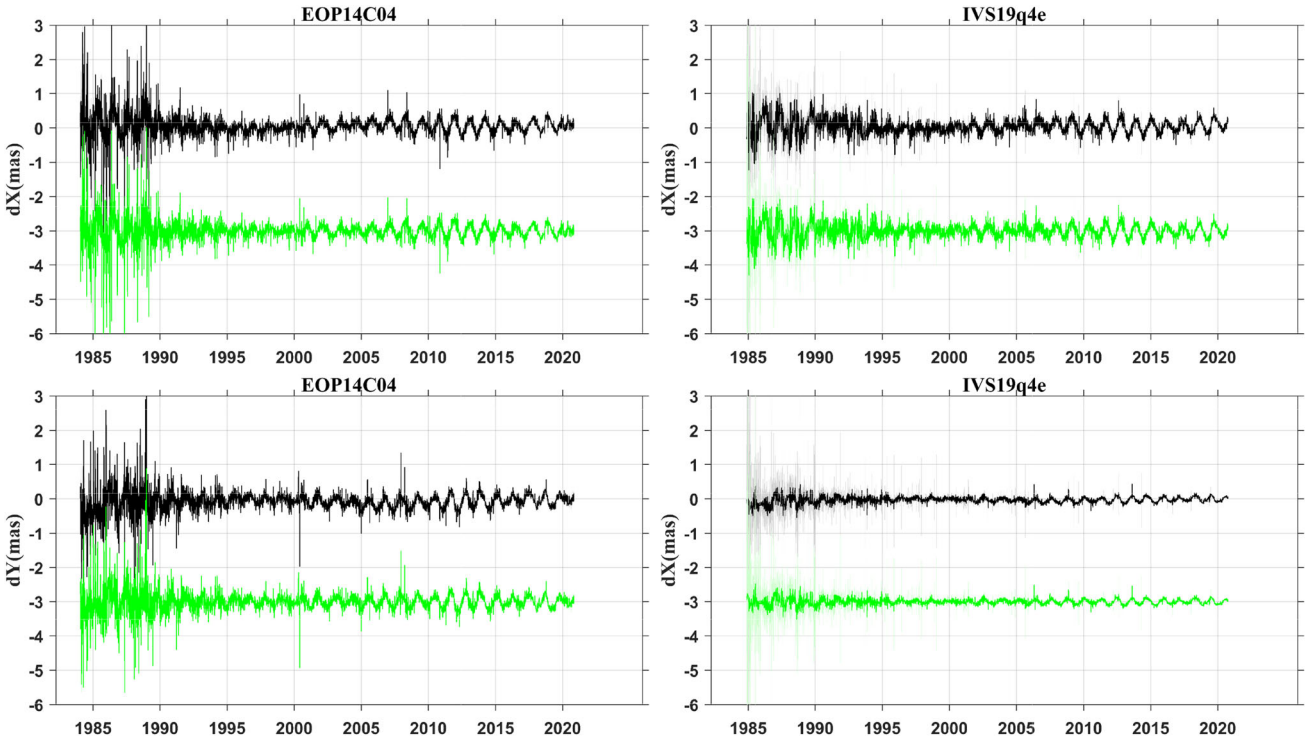

Fig. 1 The IERS 14C04 and the IVS 19q4e nutation residuals have been analyzed; black solid line is the original data from IERS and IVS, respectively, and green solid line is the residuals after applying Fits20 corrections (see Fig. 2) found in this work; a −3.0 mas offset was added to it for clarity reasons

harmonic components is about 130 μas (Gattano et al. 2017); however, in our case, we have found the weighted root mean square errors (wrms) is about 110 μas from 14C04 and 70 μas from IVS 19q4e, respectively. The wrms computed with the 14C04 and 19q4e solutions published by IERS and IVS is summarized in Table 1.

3 The corrections to the sine and cosine of coefficients the nutation term

The CIP axis in space has two type of motion: the precession and nutation. The Cartesian coordinates of this pole of the Earth's axis in the geocentric celestial reference frame are:

$$X = \psi_A + \Delta\psi \sin\varepsilon_0 \quad Y = \varepsilon_A + \Delta\varepsilon \tag{1}$$

where ψ_A and ε_A are the precession quantities in longitude and obliquity referred to the ecliptic of epoch and $\Delta\psi$, $\Delta\varepsilon$ are the nutation angles in longitude and obliquity referred to the ecliptic of epoch where ε_0 ($= 84381.40600''$) is the IAU 2006 value for the obliquity of the ecliptic at J2000.0 (Petit and Luzum 2010).

The accuracy of the equation is limited since X and Y are usually defined within the non-rotating origin convention [see IERS Conventions (Petit and Luzum 2010)], while $\Delta\psi$ and $\Delta\varepsilon$ are defined with respect to the true equinox of date and is degrading with time since the precession is measured from the intersection between the mean equator of J2000 and the ecliptic of J2000, and is in realty a combination of motions of the equator and of the ecliptic (see Dehant and Mathews 2015) to reach the mean equator of the date and the ecliptic of date. For studying the short period motions (high frequency), we can make the approximation that the precession is constant and replace $\sin\varepsilon$ by mean obliquity at J2000 so that $\sin\varepsilon_0 = 0.397777$. Then the elliptical motion can be decomposed into circular motions (Dehant and Mathews 2015):

$$\Delta\psi_n(t) = \sin\varepsilon_0(\Delta\psi_n^{\text{ip}} \sin\Phi(t) + \Delta\psi_n^{\text{oop}} \cos\Phi(t) \tag{2}$$

$$\Delta\varepsilon_n(t) = \Delta\varepsilon_n^{\text{ip}} \cos\Phi(t) + \Delta\varepsilon_n^{\text{oop}} \sin\Phi(t) \tag{3}$$

where $\Delta\psi_n$ and $\Delta\varepsilon_n$ are the amplitude coefficient of nth nutation term, the ip and oop stands for the in-phase and out-of-phase components, respectively, Φ is the argument of nutation and is mainly related to the arguments in the lunisolar potential. After application of the mean obliquity correction to the changes in longitude, the value becomes the dX of the Celestial Pole Offset (CPO), and the change in obliquity is the dY of the CPO. The observed CPO X and Y are calculated through:

$$X = \sin\varepsilon_0\Delta\psi = \sum_{i=1}^{1365}\sum_{j=1}^{19}[[A_{s_{ij}} + \dot{A}_{s_{ij}}t_i]\sin(\Phi_{ij}) + A_{c_{ij}}\cos(\Phi_{ij})] \tag{4}$$

and changes in obliquity (dY) is:

$$Y = \Delta\varepsilon = \sum_{i=1}^{1365}\sum_{j=1}^{19}[B_{s_{ij}}\sin(\Phi_{ij}) + [B_{c_{ij}} + \dot{B}_{c_{ij}}t_i]\cos(\Phi_{ij})] \tag{5}$$

where A_s and B_s are the coefficient of the sine part; the A_c and B_c are the coefficient of the cosine part. A is for $X + \mathrm{d}X$ and B is for $Y + \mathrm{d}Y$, dX and dY are the nutation residuals after removing model values, let $\mathbf{C}_x = \dot{A}_s t\sin(\Phi)$, and $\mathbf{C}_y = \dot{B}_c t\cos(\Phi)$, on substituting them in Eqs. (4) and (5), we obtain:

$$\mathbf{dX} - \mathbf{C}_x = \mathbf{A}_s\sin\Phi + \mathbf{A}_c\cos\Phi \tag{6}$$

$$\mathbf{dY} - \mathbf{C}y = \mathbf{B}_c\cos\Phi + \mathbf{B}_s\sin\Phi \tag{7}$$

In order to find the amplitudes of the 678 non-rigid Earth nutations (A_c, A_s, B_c, B_s). Equations (6) and (7) can be transformed to a linear system, $\mathbf{Ax} = \mathbf{b}$, where $\mathbf{x} = [\mathbf{A}_s\,\mathbf{A}_c]^{\mathrm{T}}$ (where T means the transpose), and $\mathbf{Ay} = \mathbf{c}$, where $\mathbf{y} = [\mathbf{B}_c\,\mathbf{B}_s]^{\mathrm{T}}$. The $\mathbf{b}$ and $\mathbf{c}$ are from the VLBI measurements and $\mathbf{A}$ is the cosine or sine coefficient matrix, which are calculated from the argument. The unknowns are the $\mathbf{x}$ and $\mathbf{y}$. The size of matrix $\mathbf{A}$ is $m \times n$, where m is the total number of observed CPOs, which increases with time, and n is the number of nutation components; here, n is equal to 678×2 for the lunisolar components. The amplitude matrices ($\mathbf{x}$, $\mathbf{y}$) can be solved through an iterative algorithm.

An iterative method is usually applied to solve square asymmetric systems, e.g., under-determined consistent systems, over-determined systems and regularized systems (Ericsson and Ruhe 1980). For $m \gg n$, this is a typical over-determined systems. The rank of matrix (r) is computed by using the singular value decomposition (svd) method (Saad 2003). A synthetic time series was generated from 20,000 (Aug. 21, 1913) to 80,000 (Nov. 28 2077) day in Modified Julian Date (MJD) with one day step. For the contribution of lunisolar origin, this forms a coefficient matrix $\mathbf{A}$ with a dimension ($120{,}002 \times 1356$). The (r) of $\mathbf{A}$ is equal to 1324. The ranks of the coefficients matrices ($\mathbf{A}$) are equal to the rank of the augmented matrices ($\mathbf{A}\ \mathbf{b}$) but smaller than the total number of unknowns (1356); therefore, the system is consistent but $\mathbf{x}$ and $\mathbf{y}$ has infinite solutions. In order to find the most likely solutions of the system ($\mathbf{A}\ \mathbf{b}$), an iterative algorithm called the Lanczos method was applied. The Lanczos method is used to solve the eigenvalue and eigenvector approximation through an iterative algorithm process. The optimized solution is found after a series of trails involving different $\mu\mathbf{B}$, supposing,

$$(\mathbf{A} - \mu\mathbf{B})\mathbf{x} = \mathbf{b} \tag{8}$$

So that $(\mathbf{A} - \mu\mathbf{B}) = \mathbf{LDL}^{\mathrm{T}}$ is factorized under the form of $\mathbf{LDL}^{\mathbf{T}}$ with triangular $\mathbf{L}$ and diagonal $\mathbf{D}$. $\mathbf{x}$ can then be solved from inverting these matrices,

$$\mathbf{x} = \mathbf{L}^{-1'}\mathbf{D}^{-1}\mathbf{L}^{-1}\mathbf{b} \tag{9}$$

According to the Lanczos method, $\mathbf{B} = \mathbf{CC}^{\mathbf{T}}$ and $\mathbf{C}$ is rectangular and is assumed to have linearly independent columns. Multiplying by $\mathbf{C}^{\mathbf{T}}$ and C the inversion of Eq. (8), ont obtains

$$(\mathbf{A} - \mu\mathbf{I})^{-1} = \mathbf{C}'(\mathbf{A} - \mu\mathbf{B})^{-1}\mathbf{C} \tag{10}$$

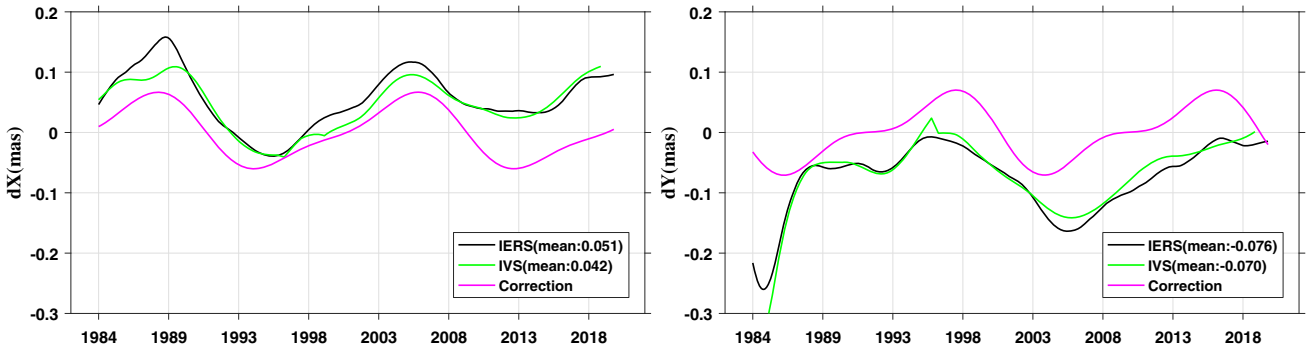

Fig. 2 The corrections for the 21 nutation components were computed for the IERS 14C04 and IVS 19q4e. We plotted two long period harmonic components (18.6 plus 9.3 yrs) and the low pass with a cutoff frequency of 8 years filtered nutation residuals of IERS and IVS. A ~ 50 μas offset and ~ -70 μas is presented in the dX and dY, respectively. The exact values of the 21 nutation components are listed at Table 4

Table 4 The unit of period is days, the positive sign is prograde motion, and negative represents retrograde one

Period	Δa_{ip}^{+}	σ	Δa_{oop}^{+}	σ	Δa_{ip}^{-}	σ	Δa_{oop}^{-}	σ
− 6798.38	4.4	3.6	55.6	5.1	9.3	2.4	− 3.4	2.4
− 3399.19	20.5	4.8	3.4	1.2	13.6	1.7	7.2	0.4
1615.75	1.9	5.0	21.0	3.7	− 1.9	1.0	− 15.7	3.6
1305.48	− 10.6	2.4	1.8	0.2	− 0.5	0.8	2.0	0.2
1095.17	− 9.4	2.3	− 1.4	0.0	− 5.0	0.6	11.1	2.3
386.00	17.4	8.0	− 8.3	0.5	− 10.4	1.8	− 15.8	4.3
365.26	12.9	3.8	− 5.3	3.9	21.3	1.8	2.7	1.2
− 346.64	12.4	4.0	− 8.5	4.2	3.5	1.2	− 11.2	0.1
182.62	− 12.3	1.9	− 14.9	3.0	− 4.7	1.0	− 0.3	0.7
121.75	− 8.5	3.4	3.0	2.2	1.1	1.0	− 9.6	0.7
31.81	− 6.3	2.4	− 2.6	1.0	− 2.3	0.7	1.6	0.5
27.56	1.3	2.1	− 2.2	1.9	− 4.3	0.7	− 15.4	0.4
23.94	0.9	3.0	− 3.1	1.7	5.0	0.8	− 3.6	0.8
14.77	− 0.8	2.8	1.9	0.5	− 1.8	0.7	4.0	0.3
13.78	1.7	1.2	0.6	0.6	− 3.9	0.8	− 0.3	0.7
13.66	9.8	1.7	− 12.7	2.4	− 13.9	1.1	− 2.3	1.2
9.56	3.4	2.6	− 1.0	1.2	1.9	0.5	− 2.2	0.5
9.13	− 4.3	3.6	3.9	1.4	0.3	0.9	1.1	0.6
9.12	− 4.2	3.5	2.6	1.0	0.4	0.8	5.2	0.4
7.10	− 3.0	4.2	− 2.0	1.2	− 1.5	0.8	− 3.2	0.2
6.86	1.8	2.5	− 1.3	0.6	0.9	0.9	0.4	0.5

The differences between amplitudes (in μas) of the major nutation component, which were fitted from each independent set of data and IAU2000 values, the errors are the standard deviation among 6 solutions

The solutions of **x** provided by Eq. (9) are searched through a range of values $[\mu_0, \mu_1, \ldots, \mu_n]$, at each trial, and similarly for **y**. A residual series is computed with a set of intermediate values of **x** and **y**. The final results were obtained when the weighted-root-mean-scattering (wrms) (Herring et al. 1986) converged, and the numerical solutions of **x** and **y** corresponding to the minimum wrms values were selected as the final results of 678 nutation components.

In our case, we use the same method to find the two times 21 corrections to the VLBI nutation series with respect to the IAU reference nutation model, based on our selected six EOP solutions. The other consideration to select these 21 terms is to avoid the interferences between correlated terms as demonstrated by our synthetic time series simulation or proofed by Petrov (2007). Because of the higher uncertainties in the CPO determinations prior to 1990 (Behrend et al. 2009), we fitted the 42 dominant nutation coefficients using the observations after 1990. We then computed the dX and dY using the corrections found here and combining them with the other nutation amplitudes from the IAU model. Figure 1 shows the original 14C04 nutation residuals and the corrected one.

The corrections for the 21 nutation terms are shown in Fig. 2 and given at Table 4. The wrms are then calculated from two sets of nutation residuals, built either using the IERS or the IVS observations, and with respect to both, the Fits20 series and the IAU2006/IAU2000A model. As seen from Fig. 3, the wrms of dX and dY are reduced significantly after 1990, which could be attributed to the fact that the quality of the VLBI measurements has been significantly improved since then. We also see in this Figure that the wrms obtained from the corrected series (Fits20) is relatively in a good agreement with the wrms computed with respect to IAU2006/IAU2000A model. However, comparing the values for all the years of both, the residuals with respect to Fits20 and the residuals about IAU2006/IAU2000a model, we found between 60 and 70% of lower value for both IERS and IVS CPO residuals computed using Fits20 series compared with the residuals computed using the IAU2006/IAU2000A model. We notice in all cases that the FCN signals are remaining in the dX and dY residuals. We treated it in the following analysis using the IERS 14C04, which provides

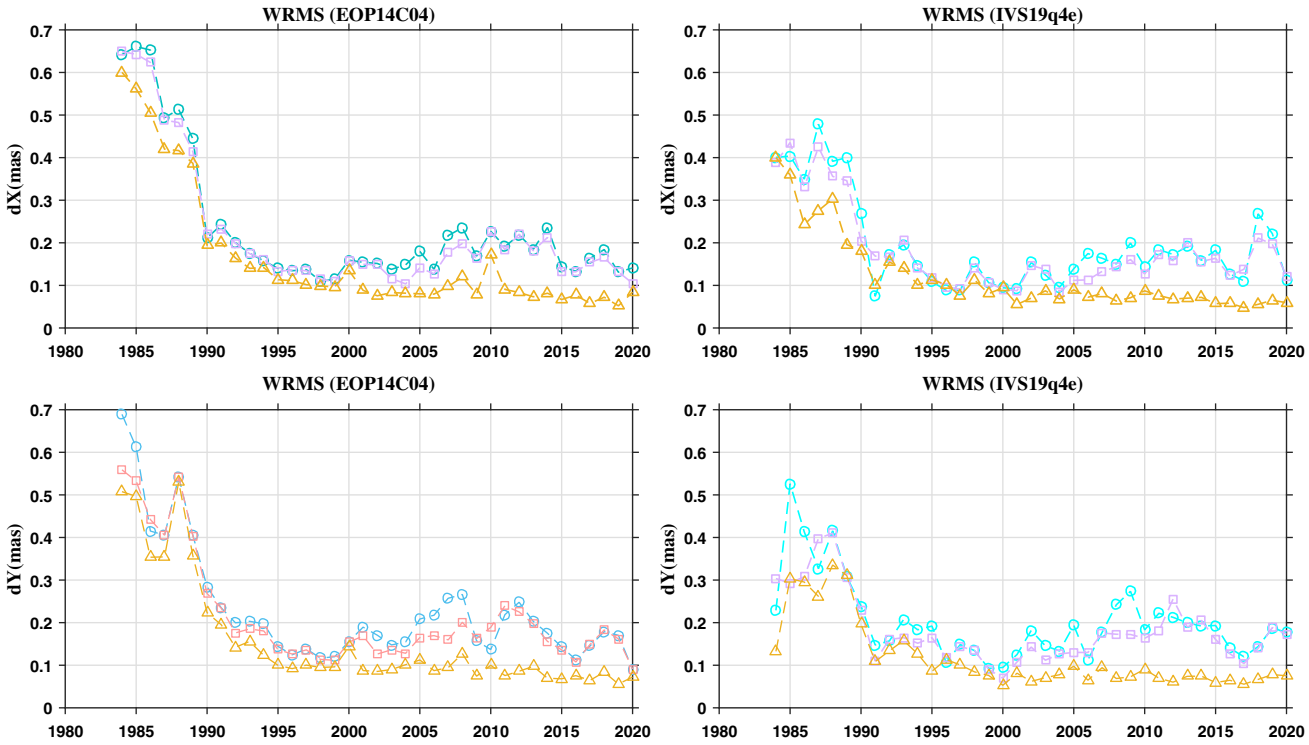

Fig. 3 The weighted-root-mean-square-errors (wrms) were computed using the IERS 14C04 and the IVS 19q4e, respectively. The residuals with respect to the IAU2006/2000A model are marked with circle, the Fits20 model is rectangular and FCN free residual is triangle

regular daily solutions of the dX and dY with respect to the IAU2006/2000A precession nutation model.

4 The free core nutation

The misalignment of the instantaneous rotation axis and figure axis produces the free core nutation (FCN) in the celestial reference frame or an nearly diurnal free wobble (NDFW) in the terrestrial reference frame. The flow inside the fluid core of the Earth is the complex result of various physical processes and phenomena including the convecting dynamo action, viscosity, etc. It is however possible to extract valuable information regarding its response to (and influence on) planetary rotation by approximating its dynamics at these timescales as that of an inviscid flow with uniform vorticity and an ellipsoidal boundary. The flow then resembles a solid body rotation around a uniform rotation vector $\omega = 2\pi/430$ (radian/day) whose orientation in time is governed by a Liouville equation analogous to that describing the rotation of the mantle. When observed from the inertial frame, this vector presents a slight misalignment with respect to the mantle rotation axis proportional to the ellipticity of the CMB. Without external tidal torque, these equation allow determining the FCN rotational normal mode with a nearly diurnal frequency (Dehant and Mathews 2015). If excited, the normal mode has a strong wobble in the fluid compared to the wobble of the Earth's mantle. This mode can be seen as a generalization of the well-known spin-over mode of fluid dynamics—which corresponds to the simplest of the inertial modes inside a rotating fluid cavity—to the case where the motion of the cavity (here the Earth) is not given a priori (Triana et al. 2019; Rekier et al. 2020). This mode is very well known in the nutation theory as it induces resonance effects in the nutation amplitudes. The transfer function for nutation (Wahr 1981), which expresses the ratio between non-rigid and rigid Earth amplitudes of the nutation, is identical to the transfer function for the non-rigid and rigid Earth amplitudes of wobbles. These transfer functions include the resonance effects of the FCN.

In order to determine the FCN from the observations, on the one hand, an empirical model can be applied to directly fit the FCN-free mode period and amplitude from VLBI-observed nutation residuals (Lambert 2006; Krásná et al. 2013; Belda et al. 2016; Gattano et al. 2017; Malkin 2013). On the other hand, the FCN period can be directly or indirectly obtained from the determination of the resonance in the nutation transfer function. For instance, the eigenperiod was directly evaluated from the nutation resonances to be between −429.8 and −432.8 solar days by Roosbeek et al. (1999). Mathews et al. (2002) and Dehant and Mathews (2015), instead, used the analytical expressions of the FCN

frequency and showed that it is depending on the flattening of the core, the couplings at the core mantle boundary and several pre-defined compliances (Mathews et al. 2002).

By fitting those parameters, the eigenperiod of FCN is found around −430 solar days. The minus sign indicates that the motion is retrograde. We are now interested in the free mode that can be excited. The atmosphere is often considered as the primary source of excitation (Lambert 2006). In this work, we consider that the eigenperiod of the FCN is established in a good agreement by estimating the physical Earth parameters using Bayesain inversion in time domain or least square analysis in frequency domain, respectively (Koot et al. 2008; Zhu et al. 2017).

In our procedure, we firstly applied the two times 21 correction terms found from the six sets of EOP solutions to the IERS 14C04 nutation residuals. The so-obtained time series are VLBI observations corrected for the best nutation model as possible. After that, we fit it to a time-varying model (Eq. 11) with a 8-year window and sliding it by a constant shift in order to represent the time dependency of the mode.

$$\begin{cases} \mathrm{d}X_{\mathrm{fcn}}(t) = A^{\mathrm{c}}_{\mathrm{fcn}} \cos(\omega_f t_i) - A^{\mathrm{s}}_{\mathrm{fcn}} \sin(\omega t_i) \;\; t_{\mathrm{s}} < t_i < t_{\mathrm{e}} \\ \mathrm{d}Y_{\mathrm{fcn}}(t) = A^{\mathrm{s}}_{\mathrm{fcn}} \cos(\omega_f t_i) + A^{\mathrm{c}}_{\mathrm{fcn}} \sin(\omega t_i) \;\; t_{\mathrm{s}} < t_i < t_{\mathrm{e}} \end{cases} \tag{11}$$

where $\mathrm{d}X_{\mathrm{fcn}}$ and $\mathrm{d}Y_{\mathrm{fcn}}$ are the time variations of the FCN in celestial X and Y pole coordinates, respectively. The $\omega_f = -2\pi/430$ radian/day is the angular frequency of the FCN and fixed, t is Julian date, t_{s} and t_{e} is the start and end date of the given window, $A^{\mathrm{c}}_{\mathrm{fcn}}$ and $A^{\mathrm{s}}_{\mathrm{fcn}}$ are the amplitudes of sine and cosine for each given moving window.

The mode in a complex plane can be expressed as $A^{\mathrm{c}}_{\mathrm{fcn}} + i\,A^{\mathrm{s}}_{\mathrm{fcn}}$, with the modulus equals to $A_{\mathrm{fcn}} = \sqrt{({A^{\mathrm{c}}_{\mathrm{fcn}}}^2 + {A^{\mathrm{s}}_{\mathrm{fcn}}}^2)}$ and the running phase $\phi_{\mathrm{fcn}} = 2a\tan(A^{\mathrm{s}}_{\mathrm{fcn}}/(A^{\mathrm{c}}_{\mathrm{fcn}} + A_{\mathrm{fcn}}))$ for a given window.The coefficient of sine and cosine components of the fitted FCN are plotted in Fig. 4. Using the method of sliding windows, we could extract both the annual and FCN amplitudes of sine and cosine from the $\mathrm{d}X$ and the $\mathrm{d}Y$.

Until now, we were speaking about a window length of several years in order to eliminate possible inferences between close nutation components and the FCN. In principle, the annual contribution has been taken out of the data by fitting the annual as one of the 21 nutations components considered in our procedure. However, this correction is fixed with time, while the atmospheric effects on nutation may change as function of the years. In order to choose the best time window among the different time windows for fitting the $A^{\mathrm{c}}_{\mathrm{fcn}}$ and $A^{\mathrm{s}}_{\mathrm{fcn}}$ (or equivalently , the real and imaginary parts of $A^{\mathrm{c}}_{\mathrm{fcn}} + i\,A^{\mathrm{s}}_{\mathrm{fcn}}$), we choose seven windows, varying from 2 to 8 years and moving it with 1 year or 1 day step (See "Appendix"). Finally, the 8-year window was selected

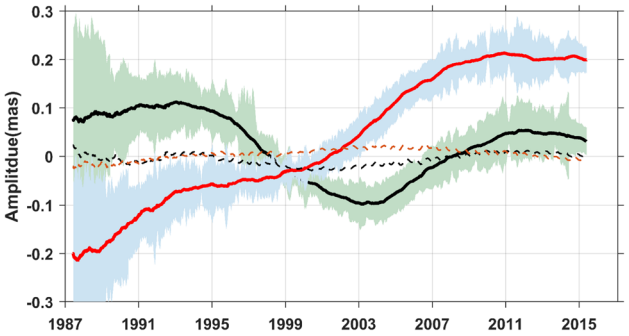

Fig. 4 The shadow area are the errors of each measurement, which are coming from the formal uncertainties of IERS 14C04 product. The amplitudes of the real (red) and the imaginary part (black) of $\mathrm{d}X + i\mathrm{d}Y$ were computed with a 8 years sliding window and moving with one day step. The dash lines are the annual nutation (S1) component

because of the remaining annual terms and the FCN are well separated and the small annual amplitude variation could be determined (see Fig. 4).

The magnitude A_{fcn} and the running phase ϕ_{fcn} of the FCN are calculated. The left-hand panel of Fig. 5 shows the magnitude of A_{fcn}. The A_{fcn} bears a 'V-shape', which reaches the minimum in 1999. The ϕ_{fcn} and A_{fcn} were plotted in a polar coordinate at the right panel. The motion of the celestial pole related to the liquid core is not strictly following a circular or ellipsoid path neither. At the beginning, it moved close to a straight line towards the east (refer to the polar map); in 1994, it had a abrupt change of the direction to the south at 120°. The crossing of 180° and 0° happened around 1998 and 2008, respectively. Another redirection occurred in 2003 at the 300°. There are three crossings: the 150–330 plane, which corresponds to 1990, 1998 and 2005. They were all coincident with the occurrence of the geomagnetic jerks which were the consequence of the rapid change of the fluid motion (Mandea et al. 2010) in a time window about 1 year in advance or behind, which were marked in the right panel in Fig. 5.

Having substituted the series of $A^{\mathrm{c}}_{\mathrm{fcn}}$ and the $A^{\mathrm{s}}_{\mathrm{fcn}}$ to Eq. (11), we generated the waveform of the FCN with a daily cadence, which resembles a negative damping before 1999 and a positive one after 1999 (Fig. 6). We used a simplified viscous damping equation $y(t) = A * e^{-\zeta\omega_f t}\sin(\sqrt{1-\zeta^2}\omega_d t + \varphi)$ (where ω_d is the damped frequency) to separately model the FCN before and after the minimum value of A_{fcn} (Fig. 7). It yields the decay rate $\zeta = 3.76 \times 10^{-4}$, $\zeta = -3.11 \times 10^{-4}$ for $\mathrm{d}X$, covering the period from 1988 to 1998 and 1999 to 2012, respectively. The value from dY is $\zeta = 1.84 \times 10^{-4}$, $\zeta = -3.03 \times 10^{-4}$ following the same convention of the $\mathrm{d}X$. From 2012 to the end of 2015, the oscillations of the $\mathrm{d}X$ and $\mathrm{d}Y$ seem to enter another phase, in which, the amplitude changes turned into a more stable stage. If we fit it with the same viscous damping

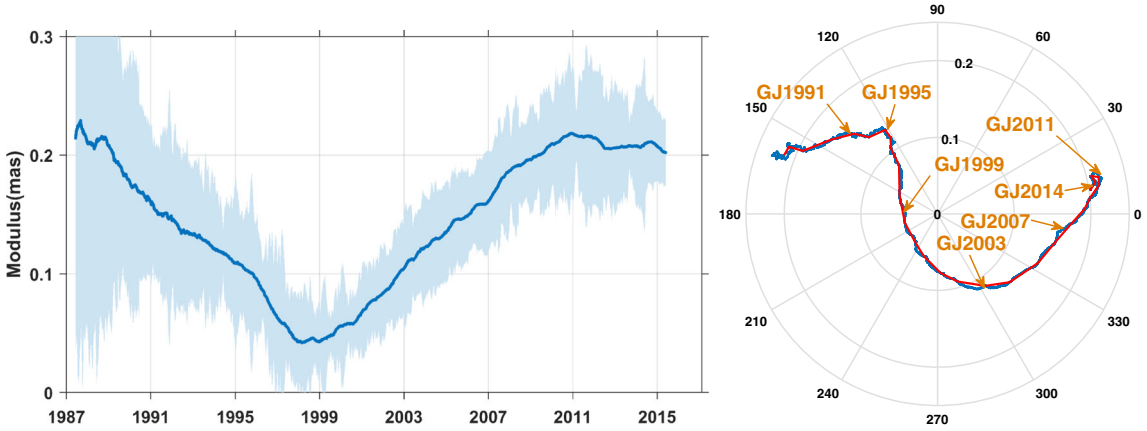

Fig. 5 The magnitude (left panel) and the phase (right panel) of FCN were computed with the real and imaginary parts of the FCN, which are plotted in Fig. 4. The red solid line in the right panel is the result with 1 year sliding step and the blue one with one day step. The errors are the normal uncertainties of the 14C04

equation, it produced the $\zeta = 2.41 \times 10^{-5}$ and 2.47×10^{-5} for the dX and dY component, which is a value more close to the one obtained from the resonance analysis (Koot et al. 2008). In Fig. 5, we compare the values of the FCN obtained by a sliding window and the ones obtained from this damping formula. If the oscillation continuously develops in this way without other perturbations, we will get a more robust result. In this case, we need at least another 4 to 5 years of additional data to confirm the new phase; this is also valid for the A_{fcn} distribution.

5 Discussion and conclusions

We have analyzed 11 sets of individual global EOP solutions and selected 6 of them to quantify the corrections of nutation terms listed in the IAU2006/IAU2000A model. Starting from these six sets of CPO residuals with respect to the IAU standard, the corrections to the amplitudes of sine and cosine components were obtained using an iterative method. After applying the corrections to the 21 nutation terms of IAU2006/IAU2000A, we generated a series called Fits20. In general, significant differences between Fits20 and the IAU2006/2000A nutation series remain in the long period wave 18.6 years, 9.3 years, the annual and the semi-annual component, which exceed their associated errors. When we compare the 21 nutation terms that we have fitted with those of Herring et al. (2002) and Mathews et al. (2002), although the results were close, they were inconsistent considering a narrow range of standard errors was determined at those frequency band. This indicates that there were still some contamination from other phenomena in the previously determined amplitudes (Herring et al. 2002). Furthermore, the corrections we found here is time-dependent (Fig. 2); thus,

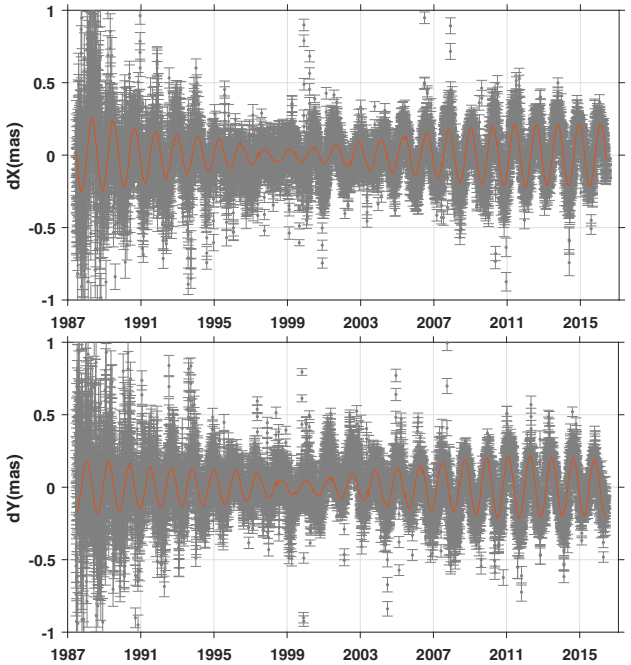

Fig. 6 The dX and dY components of the 14C04 were plotted with its associated normal uncertainties. The red solid line are the FCN signatures computed by substituting the amplitudes obtained through the sliding windows to Eq. (11)

the effect on the nutation residuals reduction are not uniform (see Fig. 3). But since those 21 nutation terms are the input of the MHB2000 nutation theory, a set of basic Earth's parameters (BEP) are inferred from the amplitude of these 21 major terms. Since the new corrections are exceed, the uncertainties of 21 nutation components determined in that model; it is worth to evaluate the BEP again. We have exercised this kind of research with 14 nutation terms by Zhu et al. (2017); however, except the imaginary part of coupling constant at

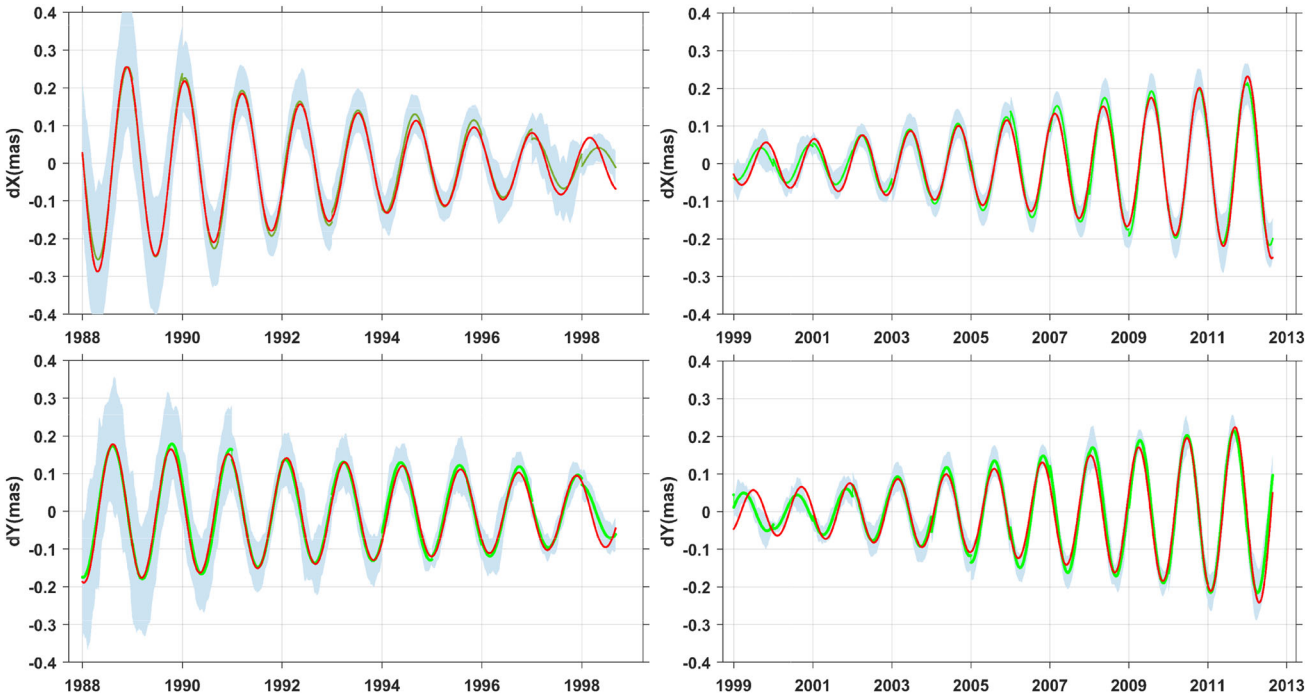

Fig. 7 The FCN signature are separated into two groups before and after 1999. The green solid line is the mode obtained from the sliding windows fitting results and the red solid line is the viscous-damping modeling to the green curve. The shaded area is the normal uncertainties of each solutions accompanied in the 14C04 solutions

the ICB shows a larger deviation, the rest of parameters are consistent with the BEP found by Mathews et al. (2002) and Koot et al. (2008); this is worth to be investigated again with corrections found in this work.

We tested our Fits20 series with respect to the IAU2006/IAU2000A model by recalculating for both the observed nutation residuals using the latest IERS EOP(14C04) combined solutions covering the period between 1984 and 2020 and the IVS (19q4e) combined solutions. The yearly wrms were computed using these two sets of CPO w.r.t. IAU2006/IAU2000A and Fits20, respectively. To be noticed, the FCN was not removed from the dX, and dY, and the formal a priori uncertainties are coming from the 14C04 and 19q4e solutions. It was essential to keep the same weights when we calculated the wrms w.r.t. both nutation series, as it guarantees that the wrms indicating deviations from the reference model but not the uncertainties of the model itself. The annual distributions of wrms are close to each other, and about 60 to 70% of these populations have lower wrms when considering Fits20 series than when considering IAU2006/IAU2000A. We computed the annual wrms again after removing the FCN from the nutation residuals about Fits20 (Fig. 3); it shows that the wrms can be minimally reduced 36%. A constant offset of $\sim +50$ μas in dX and ~ -70 μas in dY are obtained from the IERS and IVS solutions, which may be linked to the bias of the precession rate or the noise from quasars.

The FCN normal mode amplitudes were directly fitted from the nutation residuals with respect to our Fits20 model using either a sliding window or an empirical model based on damping formulation. Since the FCN is a nearly diurnal free wobble (NDFW) in the mantel frame or equivalently a period of -430 days in an inertial frame, it is close to the annual nutation. The latter one is profoundly influenced by the atmosphere and ocean with a nonlinear behavior. In order to minimize the perturbation from those terms and keep a reasonable length of data to fit the FCN, we tested different window-length from 2 to 8 years, in which the 8-year window gave the best compromise result to reduce the perturbations from the interfering frequencies (see "Appendix"). In addition, we compared the amplitudes and phases of FCN obtained in this work with the result from Krásná et al. (2013) using the same 4-year sliding windows. We must notice that Krásná et al. (2013) has used a different version of EOP solution about IAU2006/IAU2000A and another method to extract the parameters of FCN. But we have found the similar magnitude and running phases, except for a constant phase shift, as shown in "Appendix", which could be attributed to the different in the reference date of the initial value. It also suggests that the small differences between the nutation residuals computed w.r.t. IAU2006/IAU2000A and Fits20

Table 5 On the one hand, we computed the Fourier transform with the complex series of $(\mathrm{d}X + i\mathrm{d}Y)$; there are three peaks in the spectra

Method	T_1 (days)	T_0 (days)	T_1 (days)
FFT $(\mathrm{d}X + i\mathrm{d}Y)$	−397.9	−421.7	−448.7
Resonance and beating	−405.1	−430.0	−458.1

On the other hand, as if assuming that it exists, the unknown modes is beating with the FCN. From a linear approximation, we can derive the beating period $\delta = \frac{2\pi}{|\omega_0 - \omega_1|}$, given the modulation period δ is 7010 days (19.1 years) estimated from the modulus of FCN with the $T_0 = -430$ days, then the T_1 has two possible solutions (this Table). From the same analysis, we can get the modulation period from the FFT results by assigning $T_0 = -421.7$ days; if it beats with the shorter period will results a modulation period about 7008 days and with the longer period is 7050 days

are averaged out when we use the sliding windows to find the amplitude and phase of FCN. We also computed the power spectral density using the complex series $\mathrm{d}X + i\mathrm{d}Y$ generated from the corrected IERS and IVS nutation residuals (see "Appendix"). We can identify three peaks in the spectra centered at the period of −397.9, −421.7 and −458.1 days (see Table 5). This is not in an agreement with the value determined from the resonance analysis, which is also reported by Vondrak et al. (2005).

The excursion of the eigenfrequency of FCN ω_f are twofold: (1) either it could be due to the dynamic flattening of the core (Dehant et al. 2017) based on a hydrostatic or non-hydrostatic earth model with a 7.0% ω_f reduction of FCN eigenperiod in the latter case or (2) the other plausible cause is the dynamo of the Earth, but a rough estimation has found several ppm changes in ω_f needs a 20% modulation of the geomagnetic field, which is far from the reality. The nonlinear normal mode forcing could originated from the atmosphere and ocean. It could also originate from a transversal forcing from the fluid that, if existing, could enhance the beat and damping of the FCN. However, an increase of one order of magnitude in the decay rate ζ, which is only accounting for maximum a dozens ppm of ω_f shifting, translates to about several days difference in the eigenperiod.

The modulus of FCN is continuously decreasing, it took 11.2 years to reach minimum. The value is increasing steadily and reaching another peak in 12.3 years. The 3D plots of the mode looks similar to the largest and longest 18.6 years nutation (Fig. 8). Assuming it exists another resonance mode with an eigenperiod close to FCN, then the modulation period due to the beat of two close modes should be around 19 years, which is close to the 18.6 years nutation. Based on the nonlinear theory, the period of modulations depends also on the coupling between two resonant modes besides on the difference in linear frequencies. In addition, when the source of excitation behaves nonlinear, it will lead to much wider possibilities of mode interaction. In general, the engienfunctions of the modes involved are important for both linear and nonlinear coupling. Van Hoolst (2005). However, we may try to mimic the modulation from the linear approximation, which is the modulation period $\delta = \frac{2\pi}{|\omega_0 - \omega_1|}$. Let one eigenmode centered at the −430 days, assuming a beat period $\delta = 7010$ days, we can find another two possible candidate periods

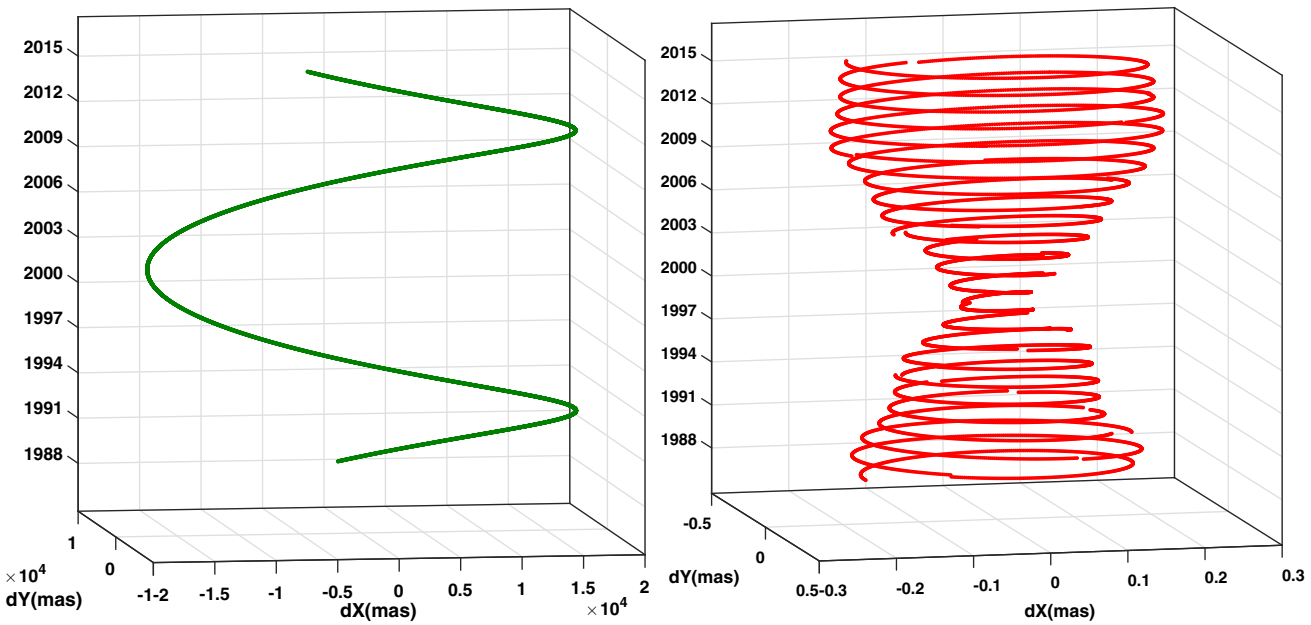

Fig. 8 The $\mathrm{d}X$ and $\mathrm{d}Y$ are plotted together in a 3D coordinate. The z-axis shows the time revolution of the long-period 18.6 years nutation and the FCN of the same period

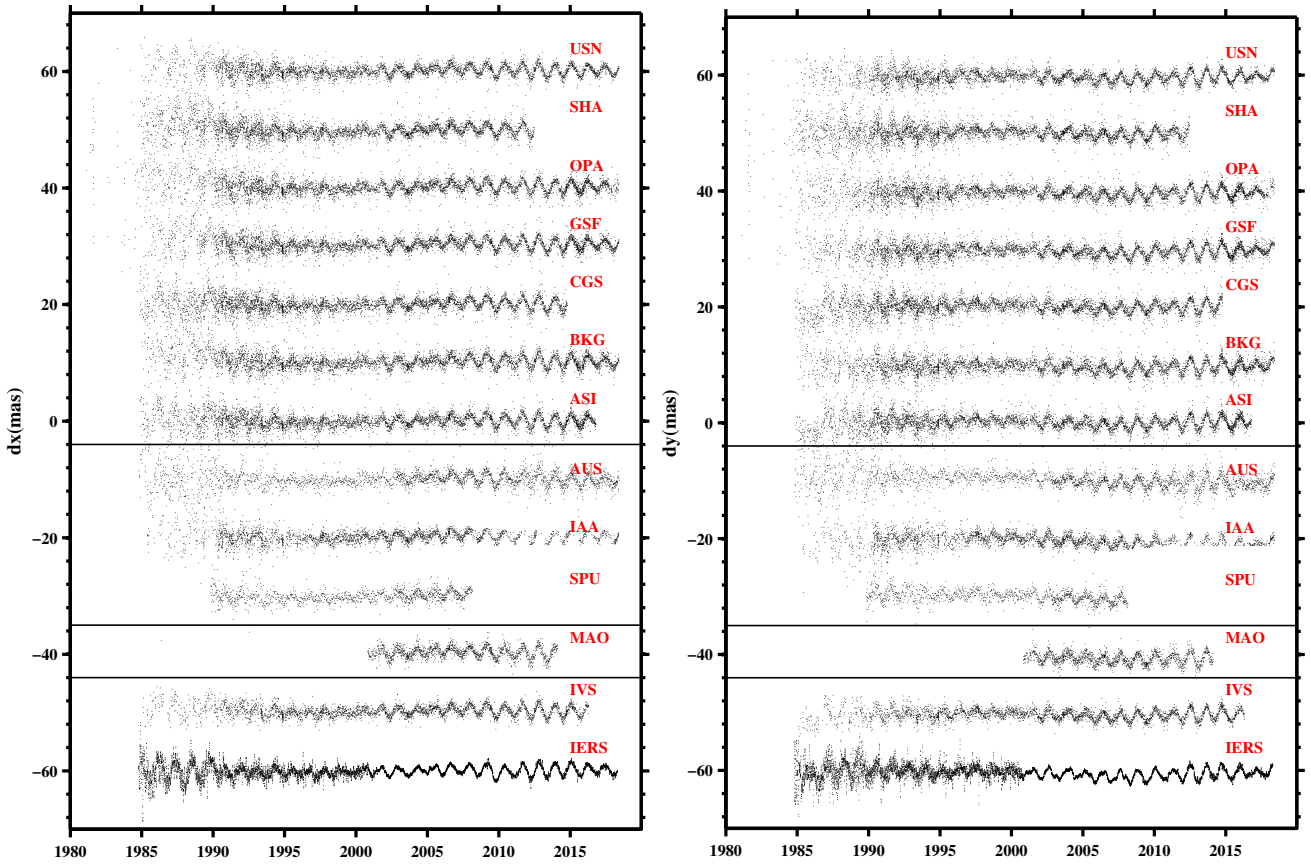

Fig. 9 Left, the celestial pole offset (CPO) dX; right, that for dY. The residuals of the CPO were computed w.r.t. the IAU2006/IAU2000A precession nutation model, and three solid lines separated the plot into four blocks. The first block contained the residuals computed by using CALC/SOLVE software, the second block contained those computed by using OCCAM software, the third block contained those computed with SteelBreeze software, and the last one contained the combined solutions by IVS and IERS. For a better demonstration of the CPO residuals, a constant amplification factor 5 was applied to the overall residuals and different offsets were added to all except ASI sets

given in Table 5. The short and long periods are −397.9 and −458.1 days, respectively. It is interesting to notice that these two modes are close to the values obtained from the Fourier transform, which hints that the modulation in A_{fcn} could be due to the interference of multiple closing eigenmodes.

If it is the case, the gaps in the FCN's eigenperiod estimation between the direct analysis (Vondrak et al. 2005) or de-convolutions method by Chao and Yikai (2015) and the indirect resonance (Hinderer et al. 2000; Dehant et al. 2003) one could be closed. The modeling of the nonlinear reactions of the free mode to an external driving mechanism will improve our knowledge about the coupling and viscosity of the core, which will in turn benefit a better understanding the various transient events, such as the geomagnetic jerks, which has been suggested by several studies (Vondrak et al. 2005; Shirai et al. 2005; Malkin 2013); the FCN's parameters may be sensitive to this sudden acceleration of the fluid core manifested as the geomagnetic jerks. However the polar form of the complex expression of FCN showed in Fig. 5 seems to confirm such a correlation, but a physical mechanism of excitation remains absent.

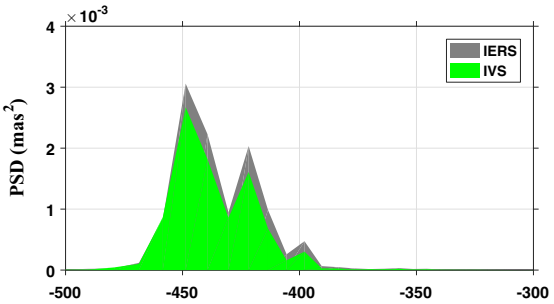

Fig. 10 The PSD was computed with the complex number (d$X + i$dY) constructed with the IERS and IVS solutions

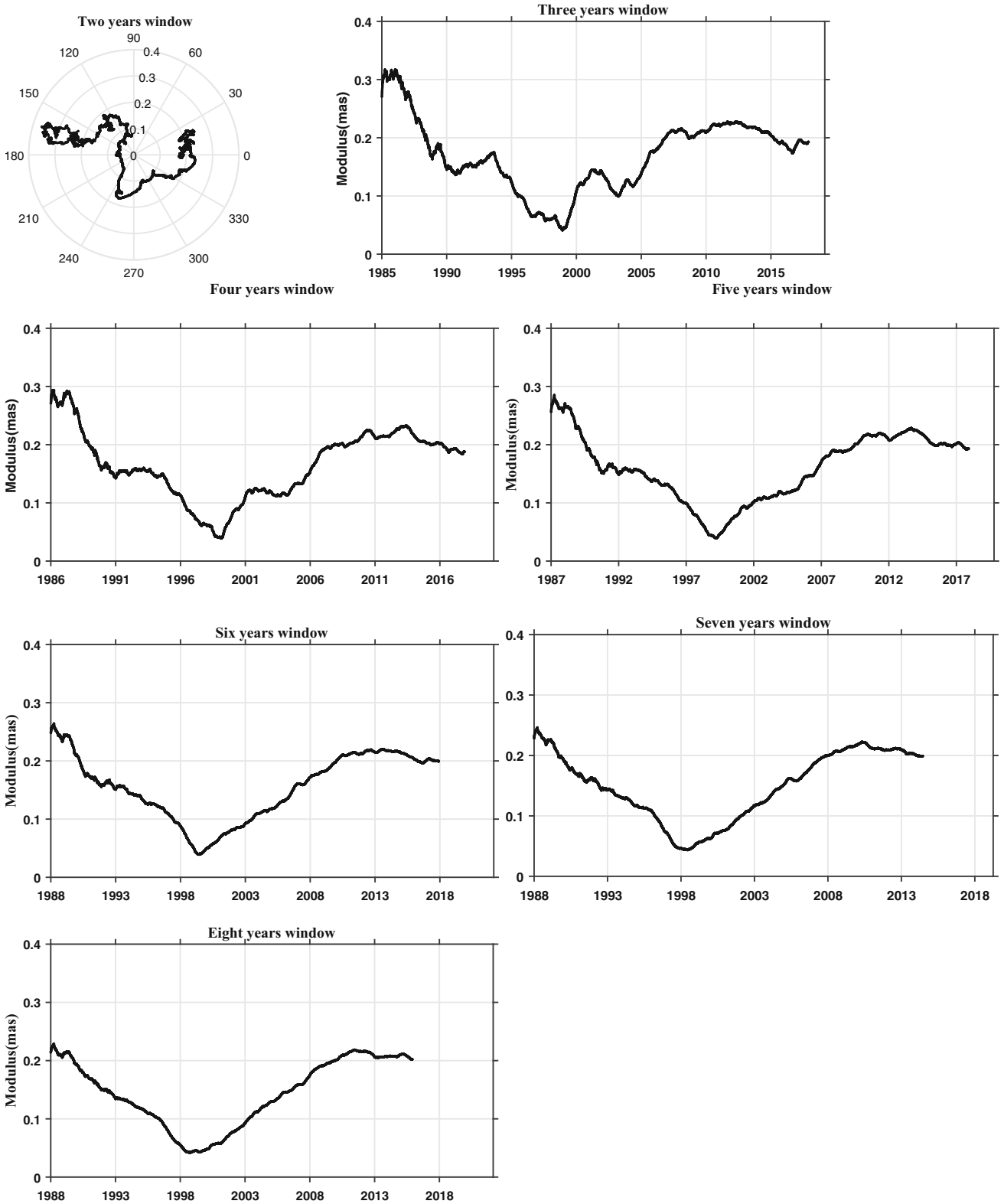

Fig. 11 We used different windows to fit the amplitude of sine and cosine of the FCN. In order to increase the time resolution, one day sliding step is adopted. The result shows the small oscillation are step by step removed by increasing the length of the window

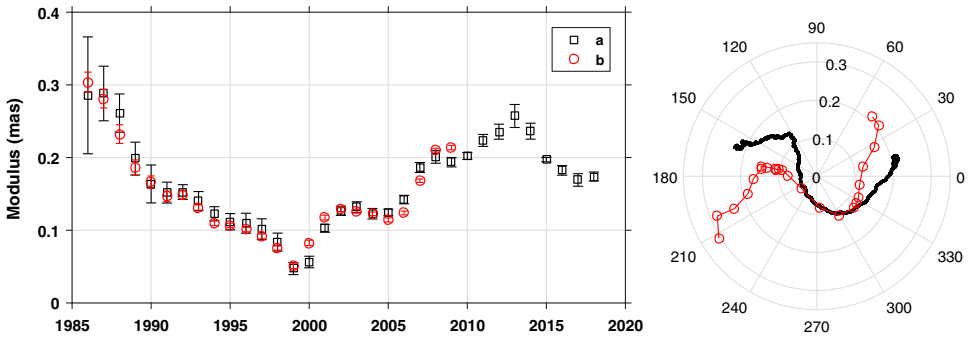

Fig. 12 The FCN magnitude and phase were calculated from the 4-year sliding windows (**a**); it is compared with results published by Krásná et al. (2013) (**b**)

Acknowledgements The authors are grateful to anonymous reviewers for their careful reading of our manuscript and their many insightful comments and suggestions. This study was supported by the ERC Grant ROTANUT (670874) and GRACEFUL (855677).

Author Contributions PZ has developed the Earth NuTAtion code and written the overall manuscript. SAT, JR and AT have contributed to the verification of the code, the description and the discussion part of FCN. VD has joined the analysis and polished the complete manuscript.

Data availibility The IERS 14C04 EOP solution are available from the IERS website (http://www.iers.or) and the IVS 19q4e is accessible through http://cddis.nasa.gov All processed data and Fis20 series and the nutation series developed in the past are accessible through http://gitlab-as.oma.be/zhuping/earths-nutation.

A Appendix

The 11 sets of EOP solutions are used to estimate the uncertainties of the 21 nutation component are showed in Fig. 9.

We computed the power spectral density with the complex number $(\mathrm{d}X + i\mathrm{d}Y)$ built from the IERS and IVS corrected residuals (Fig. 10), which partly explains the diversity of the eigen-period of the FCN found by different studies. One possible interpretation about the wider δT is that the eigen-period and phase of FCN may be changed due to the rotation of the Earth as indicated by Krásná et al. (2013), which hints a splitting of the mode; however, this need be investigated further.

We tested different window lengths starting from 2 to 8 years (Fig. 11) and compared the results with 4 years time window (Fig. 12). The amplitude of the short-term oscillations were decreasing with the increasing of the length of the window. The time reference is the mid point of each window. We used a one day sliding step to track the time variation of the mode.

References

Altamimi Z, Rebischung P, Métivier L, Collilieux X (2016) ITRF2014: a new release of the international terrestrial reference frame modeling nonlinear station motions. J Geophys Res Solid Earth 121(8):6109–6131. https://doi.org/10.1002/2016JB013098

Behrend D, Böhm J, Charlot P, Clark T, Corey B, Gipson J, Haas R, Koyama Y, MacMillan D, Malkin Z et al (2009) Recent progress in the VLBI2010 development. In: Sideris MG (ed) Observing our changing earth. Springer, Berlin, pp 833–840. https://doi.org/10.1007/978-3-540-85426-5_96

Belda S, Ferrandiz JM, Heinkelmann R, Nilsson T, Schuh H (2016) Testing a new free core nutation empirical model. J Geodyn 94:59–67. https://doi.org/10.1016/j.jog.2016.02.002

Belda S, Heinkelmann R, Ferrándiz JM, Karbon M, Nilsson T, Schuh H (2017) An improved empirical harmonic model of the celestial intermediate pole offsets from a global VLBI solution. Astron J 154(4):166

Bizouard C, Lambert S, Becker O, Richard JY (2018) The IERS EOP 14C04 solution for Earth orientation parameters consistent with ITRF 2014. J Geod 2018:1–13

Bretagnon P, Francou G, Rocher P, Simon J (1998) Smart97: a new solution for the rotation of the rigid Earth. Astron Astrophys 329:329–338

Capitaine N, Wallace PT, Chapront J (2003) Expressions for IAU 2000 precession quantities. Astron Astrophys 412(2):567–586. https://doi.org/10.1051/0004-6361:20031539

Chao BF, Yikai H (2015) The Earth's free core nutation: formulation of dynamics and estimation of eigenperiod from the very-long-baseline interferometry data. Earth Planet Sci Lett 432:483–492

Charlot P, Jacobs CS, Gordon D, Lambert Sébastien, de Witt A, Böhm J, Fey AL, Heinkelmann R, Skurikhina E, Titov O et al (2020) The third realization of the International Celestial Reference Frame by very long baseline interferometry. A&A 644:A159

Dehant V, Mathews PM (2015) Precession, nutation and wobble of the earth. Cambridge University Press, Cambridge

Dehant V, Feissel-Vernier M, de Viron O, Ma C, Yseboodt M, Bizouard C (2003) Remaining error sources in the nutation at the submilliarc second level. J Geophys Res Solid Earth. https://doi.org/10.1029/2002JB001763

Dehant V, Laguerre R, Rekier J, Rivoldini A, Triana SA, Trinh A, Van Hoolst T, Zhu P (2017) Understanding the effects of the core on the nutation of the Earth. Geod Geodyn. https://doi.org/10.1016/j.geog.2017.04.005

Ericsson T, Ruhe A (1980) The spectral transformation Lanczos method for the numerical solution of large sparse generalized symmetric eigenvalue problems. Math Comput 35(152):1251–1268

Gattano C, Lambert SB, Bizouard C (2017) Observation of the earth's nutation by the VLBI: how accurate is the geophysical signal. J Geod 91(7):849–856. https://doi.org/10.1007/s00190-016-0940-7

Hartmann T, Soffel M, Ron C (1999) The geophysical approach towards the nutation of a rigid Earth. Astron Astrophys Suppl Ser 134(2):271–286

Herring T, Gwinn C, Shapiro I (1986) Geodesy by radio interferometry: Studies of the forced nutations of the Earth: 1. Data analysis. J Geophys Res Solid Earth 91(B5):4745–4754

Herring T, Buffett B, Mathews P, Shapiro I (1991) Forced nutations of the earth: Influence of inner core dynamics: 3. Very long interferometry data analysis. J Geophys Res Solid Earth 96(B5):8259–8273

Herring T, Mathews P, Buffett B (2002) Modeling of nutation–precession: very long baseline interferometry results. J Geophys Res Solid Earth. https://doi.org/10.1029/2001JB000165

Hinderer J, Boy JP, Gegout P, Defraigne P, Roosbeek F, Dehant Véronique (2000) Are the free core nutation parameters variable in time? Phys Earth Planet Interiors 117:37–49

Kinoshita H (1977) Theory of the rotation of the rigid Earth. Celest Mech 15(3):277–326

Koot L, Rivoldini A, de Viron O, Dehant V (2008) Estimation of Earth interior parameters from a bayesian inversion of very long baseline interferometry nutation time series. J Geophys Res Solid Earth. https://doi.org/10.1029/2007JB005409

Krásná H, Böhm J, Schuh H (2013) Free core nutation observed by VLBI. Astron Astrophys 555:A29. https://doi.org/10.1051/0004-6361/201321585.371-374

Lambert S (2006) Atmospheric excitation of the Earth's free core nutation. Astron Astrophys 457(2):717–720. https://doi.org/10.1051/0004-6361:20065813

Malkin Z (2013) Free core nutation and geomagnetic jerks. J Geodyn 72:53–58. https://doi.org/10.1016/j.jog.2013.06.001

Mandea M, Holme R, Pais A, Pinheiro K, Jackson A, Verbanac G (2010) Geomagnetic jerks: rapid core fild variations and core dynamics. Space Sci Rev 155:147–175. https://doi.org/10.1007/s11214-010-9663-x

Mathews P, Herring T, Buffett B (2002) Modeling of nutation and precession: new nutation series for nonrigid earth and insights into the Earth's interior. J Geophys Res Solid Earth. https://doi.org/10.1029/2001JB000390

Petit G, Luzum B (2010) IERS Conventions, Verlag des Bundesamts für Kartographie und Geodäsie Frankfurt am Main 2010, pp 56–58

Petrov L (2007) The empirical Earth rotation model from VLBI observations. A&A 467:359–369

Rekier J, Triana SA, Trinh A, Dehant V (2020) Inertial modes of a freely rotating ellipsoidal planet and their relation to nutations. (**Accepted to appear in PSJ**)

Roosbeek F, Dehant V (1998) RDAN97: an analytical development of rigid Earth nutation series using the torque approach. Celest Mech Dyn Astron 70(4):215–253

Roosbeek F, Defraigne P, Feissel M, Dehant V (1999) The free core nutation period stays between 431 and 434 sidereal days. Geophys Res Lett 26:131–134

Saad Y (2003) Iterative methods for sparse linear systems. SIAM, Philadelphia

Seidelmann P (1982) 1980 IAU theory of nutation: the final report of the IAU working group on nutation. Celest Mech 27(1):79–106

Shirai T, Fukushima T, Malkin Z (2005) Detection of phase disturbances of free core nutation of the Earth and their concurrence with geomagnetic jerks. Earth Planets Space 57:151–155

Soffel M, Klioner SA, Petit G, Wolf P, Kopeikin SM, Bretagnon P, Brumberg VA, Capitaine N, Damour T, Fukushima T et al (2003) The IAU2000 resolutions for astrometry, celestial mechanics, and metrology in the relativistic framework: explanatory supplement. Astron J 126(6):2687–2706

Souchay J, Loysel B, Kinoshita H, Folgueira M (1999) Corrections and new developments in rigid earth nutation theory—III. Final tables. Astron Astrophys Suppl Ser 135(1):111–131

Triana SA, Rekier J, Trinh A, Dehant V (2019) The coupling between inertial and rotational eigenmodes in planets with liquid cores. Geophys J Int 218(2):1071–1086. https://doi.org/10.1093/gji/ggz212

Van Hoolst T (2005) Resonances between two stellar oscillation modes with nearly equal frequencies. A&A 295:371–392

Vondrak J, Weber R, Ron C (2005) Free core nutation: direct observations and resonance effects. A&A 444(1):297–303

Wahr J (1981) The forced nutations of an elliptical, rotating, elastic and oceanless earth. Geophys J Int 64(3):705–727

Zhu S, Groten E, Reigber C (1990) Various aspects of numerical determination of nutation constants. II—an improved nutation series for the deformable earth. Astron J 99:1024–1044

Zhu P, Rivoldini A, Koot L, Dehant V (2017) Basic earth's parameters as estimated from VLBI observations. Geod Geodyn 8(6):427–432. https://doi.org/10.1016/j.geog.2017.04.007 +++

Zhu P, Triana AS, Rekier J, Trinth A, Dehant V, Rotanut team (2020) EarTh's NutAtion computation packages (ETNA). https://doi.org/10.24414/mrh3-fc03